Distribution of 1-(2-Deoxy-2-fluoro-β-D-arabinofuranosyl) Uracil in Mice Bearing Colorectal Cancer Xenografts: Rationale for Therapeutic Use and as a Positron Emission Tomography Probe for Thymidylate Synthase

Julie L. Eiseman,[1,2] Clive Brown-Proctor,[3] Paul E. Kinahan,[3] Jerry M. Collins,[5] Lawrence W. Anderson,[5] Erin Joseph,[1] Deborah R. Hamburger,[1] Su-shu Pan,[1,2] Chester A. Mathis,[3] Merrill J. Egorin,[1,2,4] and Raymond W. Klecker[5]

[1]Molecular Therapeutics/Drug Discovery Program, University of Pittsburgh Cancer Institute, Pittsburgh, Pennsylvania; [2]Department of Pharmacology, [3]Department of Radiology, and [4]Division of Hematology/Oncology, Department of Medicine, University of Pittsburgh School of Medicine, Pittsburgh, Pennsylvania; and [5]Laboratory of Clinical Pharmacology, Food and Drug Administration, Rockville, Maryland

ABSTRACT

Purpose: **In colorectal, breast, and head and neck cancers, response to 5-fluorouracil is associated with low expression of thymidylate synthase. In contrast, tumors with high expression of thymidylate synthase may be more sensitive to prodrugs such as 1-(2-deoxy-2-fluoro-β-D-arabinofuranosyl) uracil (FAU) that are activated by thymidylate synthase. These studies were designed to evaluate FAU as a potential therapeutic and diagnostic probe.**

Experimental Design: **[^{18}F]-FAU and [^{3}H]-FAU were synthesized with >97% radiochemical purity. [^{3}H]-FAU or [^{18}F]-FAU was administered intravenously to severe combined immunodeficient mice bearing either HT29 (low thymidylate synthase) or LS174T (high thymidylate synthase) human colon cancer xenografts. Four hours after [^{3}H]-FAU dosing, tissue distribution of total radioactivity and incorporation of 1-(2-deoxy-2-fluoro-β-D-arabinofuranosyl) 5-methyluracil (FMAU), derived from thymidylate synthase activation of FAU, into tumor DNA was measured. Positron emission tomography (PET) images were obtained for 90 minutes after injection of [^{18}F]-FAU. Thymidylate synthase activity was determined *in vitro* in tumors from untreated mice by [^{3}H] release from [^{3}H]dUMP. Each cell line was incubated *in vitro* with [^{3}H]-FAU or [^{3}H]-FMAU in the absence or presence of 5-fluoro-2′-deoxyuridine (FdUrd) and then was analyzed for incorporation of radiolabel into DNA.**

Results: **Thymidylate synthase enzymatic activity in LS174T xenografts was ~3.5-fold higher than in HT29 xenografts, and incorporation of radioactivity derived from [^{3}H]-FAU into LS174T DNA was ~2-fold higher than into HT29 DNA. At 240 minutes, radioactivity derived from [^{3}H]-FAU was ~2-fold higher in tumors than in skeletal muscle. At times up to 90 minutes, PET imaging detected only small differences in uptake of [^{18}F]-FAU between the tumor types. Fluorine-18 in skeletal muscle was higher than in tumor for the first 90 minutes and plateaued earlier, whereas [^{18}F] in tumor continued to increase during the 90-minute imaging period. For both cell lines *in vitro*, FdUrd decreased the rate of incorporation of [^{3}H]-FAU into DNA, whereas the incorporation of [^{3}H]-FMAU was increased.**

Conclusions: **These results for FAU incorporation into DNA *in vitro* and *in vivo* further support clinical evaluation of FAU as a therapeutic agent in tumors with high concentrations of thymidylate synthase that are less likely to respond to 5-fluorouracil treatment. The high circulating concentrations of thymidine reported in mice may limit their utility in evaluating FAU as a PET probe.**

INTRODUCTION

Drugs, such as 5-fluorouracil (5FU) and floxuridine, that target thymidylate synthase, and hence, DNA synthesis, have been marginally active in the treatment of breast, colorectal, and head and neck cancer (1). Increased expression of thymidylate synthase has been one of the major factors associated with resistance to these agents and with a poor clinical outcome, especially for colorectal cancer (2–5).

New treatment strategies are needed to treat thymidylate synthase inhibitor-resistant tumors. Moreover, the availability of a positron emission tomography (PET) probe that could identify tumors with a high thymidylate synthase phenotype should facilitate identification of patients for whom thymidylate synthase inhibitors are more or less likely to be effective therapies. In studies described previously (6), we proposed that, instead of inhibiting thymidylate synthase, it was possible to use high catalytic activity of thymidylate synthase to activate deoxyuridine prodrugs to toxic products that would be incorporated into

Received 12/5/03; revised 6/17/04; accepted 6/24/04.
Grant support: Supported in part by American Cancer Society, George Heckman Institutional Research Grant, University of Pittsburgh Cancer Institute, and National Cancer Institute, NIH, 2P30CA47904.
The costs of publication of this article were defrayed in part by the payment of page charges. This article must therefore be hereby marked *advertisement* in accordance with 18 U.S.C. Section 1734 solely to indicate this fact.
Note: C. Brown-Proctor is currently with Pfizer Corporation, Ann Arbor, Michigan; P. Kinahan is currently in the Department of Radiology, University of Washington School of Medicine, Seattle, Washington.
Requests for reprints: Julie Eiseman, University of Pittsburgh Cancer Institute, UPCI Research Pavilion, The Hillman Cancer Center G.27B, 5117 Centre Avenue, Pittsburgh, PA 15213-1863. Phone: (412) 623-3239; Fax: (412) 623-1212; E-mail: eisemanj@msx.upmc.edu.

DNA and act as suicide inhibitors of cell growth. The drug 1-(2-Deoxy-2-fluoro-β-D-arabinofuranosyl) uracil (FAU) is the prototype for this class of deoxyuridine prodrugs.

In several cancer cell lines, FAU was phosphorylated intracellularly to its monophosphate, 1-(2-deoxy-2-fluoro-β-D-arabinofuranosyl) uracil monophosphate (FAUMP), by thymidine kinase and methylated in the 5-position by thymidylate synthase to form the product, 1-(2-deoxy-2-fluoro- β-D-arabinofuranosyl) 5-methyluracil monophosphate (FMAUMP; Fig. 1). In the work presented here, we have extended these *in vitro* studies to xenograft models to evaluate whether FAU would be incorporated preferentially into the tumor and whether [^{18}F]-FAU could be used to image tumors that have high thymidylate synthase catalytic activity. Specifically, we (*a*) examined the distribution of [^{3}H]-FAU and its metabolites in severe combined immunodeficient (SCID) mice bearing one of two human colon cancer xenografts, HT29, which has low thymidylate synthase catalytic activity, or LS174T, which has high thymidylate synthase catalytic activity; (*b*) examined thymidylate synthase catalytic activity in the tumors and incorporation of radioactivity derived from [^{3}H]-FAU into tumor DNA; (*c*) synthesized [^{18}F]-FAU and evaluated its usefulness as a PET imaging agent; and (*d*) evaluated the relative role of thymidylate synthase *versus* other pathways for these two cell lines by monitoring changes in incorporation into DNA when thymidylate synthase was inhibited.

The data presented suggest that FAU may be a useful prodrug for the treatment of tumors with high thymidylate synthase catalytic activity. The potential utility of [^{18}F]-FAU as a PET probe for thymidylate synthase was difficult to assess fully from these studies.

MATERIALS AND METHODS

Animals. Female C.B-17 SCID mice (specific-pathogen-free, 4–5 weeks of age) were purchased from Taconic Farms (Germantown, NY) and allowed 1 week to acclimate to the Animal Facilities at the University of Pittsburgh. To minimize exogenous infection, we maintained mice in microisolator cages in a separate room and handled them in accordance with the Guide for the Care and Use of Laboratory Animals (National Research Council, National Academy of Sciences, 1996) and on a protocol approved by the University of Pittsburgh Animal Care and Use Committee. Ventilation and air flow in the Animal Facility were greater than 12 changes/h. Room temperature was regulated at 72 ± 2°F. Mice received Prolab IsoPro RMH 3000 Irradiated Lab Diet and autoclaved water *ad libitum*. Sentinel mice maintained in the same room in caging containing one fifth of the bedding from study mice remained murine antibody profile-negative (MAP, Charles River, Kingston, NY), which indicated that study mice were specific-pathogen-free throughout the study period.

Tumors. HT29 cells were obtained from the National Cancer Institute, Tumor Repository (Frederick, MD), and LS174T cells were obtained from American Type Culture Collection (Manassas, VA). Cells were maintained in RPMI 1640 (Life Technologies, Inc., Invitrogen Corp, Carlsbad, CA) supplemented with 10% fetal bovine serum (Biofluids, Rockville, MD) and 10 μg/mL gentamicin (Life Technologies, Inc.) in a humidified incubator at 5% CO_2 and 37°C. Cells and fragments of both tumors from mouse-passaged tumors were placed in dimethylsulfoxide-fetal bovine serum-RPMI 1640 (10:15:75, v/v/v) and were stored in liquid nitrogen until implantation into passage mice. Both tumor lines were murine antibody profile-negative. Tumors from passage mice were harvested, cut into 25-mg fragments, and implanted subcutaneously on the right flank of study mice. Tumors in mice were measured twice weekly by digital caliper and tumor volumes (*V*) were calculated by the formula, $V = L \times W^2/2$, where length (*L*) is the longest diameter and width (*W*) is the shortest diameter perpendicular to length. When the subcutaneous tumors measured between 500 and 2000 mm^3, mice were allocated into groups such that the means and medians of each treatment group were similar. Tumor doubling time was calculated as the number of days required for each tumor to grow from 200 to 400 mm^3.

[^{18}F]-FAU Synthesis. The synthetic scheme, modified from the method of Mangner *et al.* (7), is illustrated in Fig. 2. α-D-ribofuranose 1,3,5-tribenzoate (Aldrich; Milwaukee, WI) was the starting material for preparation of protected trifyl precursor **1** (Fig. 2; 10 mg, 16.8 μmol), which was dissolved in

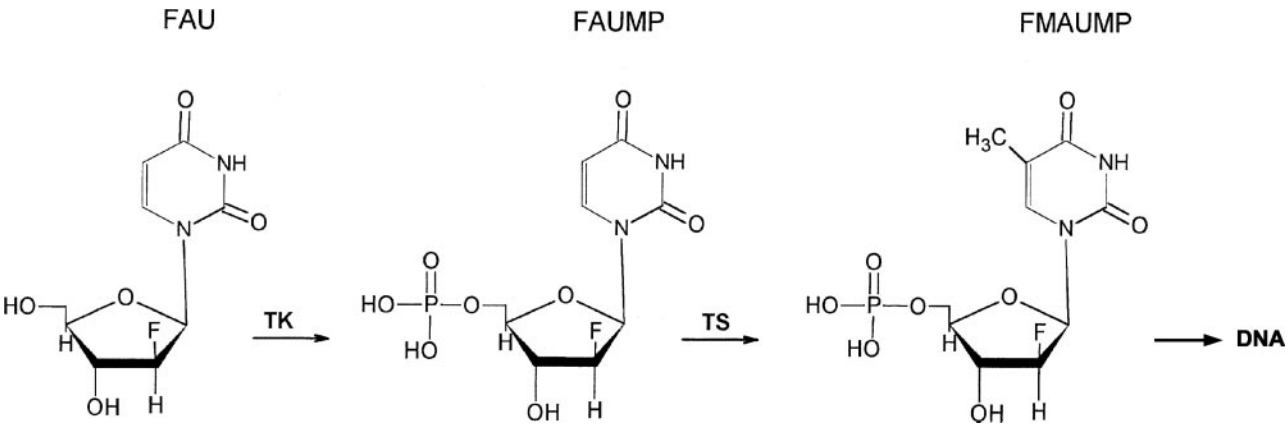

Fig. 1 Metabolic pathway. After initial phosphorylation by thymidine kinase (*TK*), methylation via thymidylate synthase (TS) is required for incorporation of FAU into DNA.

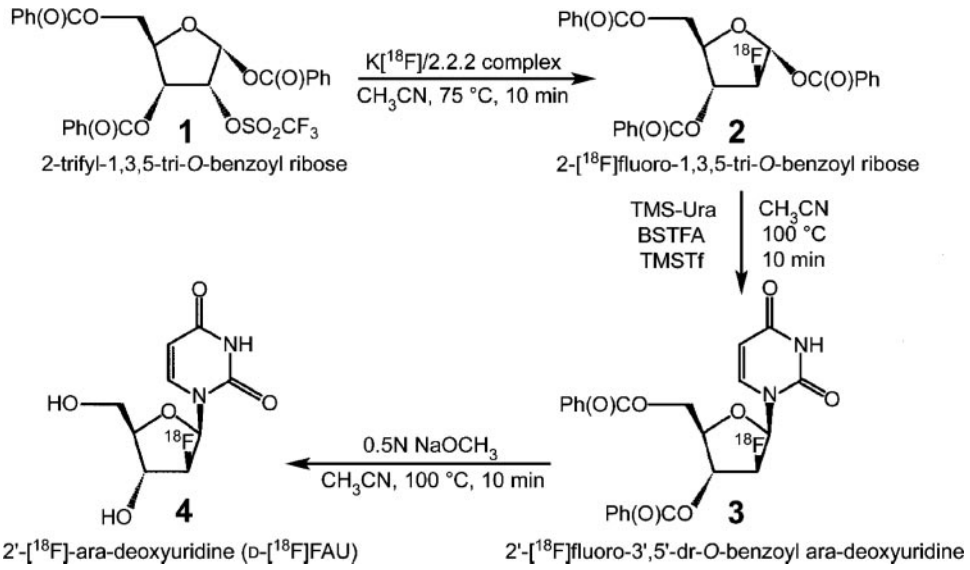

Fig. 2 Synthetic method for preparation of [^{18}F]-FAU. *TMS-Ura*, bis(trimethylsilyl) uracil. *BSTFA*, bis(trimethylsilyl) trifluoroacetamide; *TMSTf*, trimethylsilyl trifluoromethane sulfonate.

1 mL of anhydrous acetonitrile and added to a reaction V-vial containing [^{18}F]fluoride prepared in an aminopolyether support by the Hamacher method (8). The vial was sealed, and the reaction mixture was heated at 75°C for 10 minutes. The crude reaction mixture was injected onto a Prodigy 10-μm C18 octadecylsilane (ODS; ref. 3) high-performance liquid chromatography (HPLC) column (250 mm × 10 mm inner diameter, Phenomenex U.S.A., Torrance, CA) and was eluted with acetonitrile–triethylamine buffer (pH 7.3), 65:35 (v/v), at flow rates of 5 mL/min (0–12 minutes) and 9 mL/min (12–25 minutes). The radioactive peak corresponding to the desired reaction intermediate **2** (Fig. 2; t_R = 20 minutes) was diverted to a pressure reservoir containing triethylamine buffer, 250 mL. The resulting solution was then passed across two C18 Plus Sep Pak cartridges (Waters, Millford, MA) connected in series. Product **2** (Fig. 2) was collected in a fresh V-vial by passage of acetonitrile (500 μL) across the Sep Pak. Trimethylsilyl triflate (10 μL), bis(trimethylsilyl) trifluoroacetamide (10 μL), and bis(trimethylsilyl) uracil were added to the solution of **2**, and the vial was sealed and heated at 100°C for 10 minutes. The crude product **3** (Fig. 2) from this reaction was identified by HPLC in an aliquot of the reaction mixture. Deprotection of the benzoyl moieties was then affected by addition of sodium methoxide (200 μL, 0.5 mol/L in methanol) and heating at 100°C for 10 minutes. The final product (D-[^{18}F]-FAU, product **4**, Fig. 2) was then isolated from the crude reaction mixture after removal of acetonitrile by evaporation. To accomplish this isolation, preparative HPLC was done with a Phenomenex Aqua 5-μm C18 200 column (250 mm × 4.6 mm) and a flow rate of 1.2 mL/min for the mobile phase, EtOH–50 mmol/L phosphate buffer, 2.5:97.5 (v/v). An aliquot of the final product was coinjected with a standard sample of unlabeled product **4** (Moravek Biochemicals, Brea, CA) onto a Phenomenex Aqua analytical HPLC column (220 mm × 4.6 mm) and was eluted at a flow rate of 1 mL/min for the mobile phase, acetonitrile: 50 mmol/L phosphate buffer, 5:95 (v/v). The compounds coeluted (t_R = 13 minutes). Product **4** was thereby isolated in 99% radiochemical purity and 3% radiochemical yield. Specific activity of [^{18}F]-FAU was 811 Ci/mmol.

6-[^{3}H]-FAU was prepared from 6-[^{3}H]uracil (11 Ci/mmol, Moravek) by the method of Mangner *et al.* (7), except that the starting material (Fig. 2, *product 2*) was obtained directly from Sigma (Sigma Chemical Co., St. Louis, MO) and not labeled with [^{18}F]. [^{3}H]-FAU was suspended in 0.9% NaCl (Baxter Healthcare Corp., Deerfield, IL) such that each milliliter contained 42 μCi/mL.

Tissue Distribution Studies. Three mice bearing HT29 tumors and three mice bearing LS174T tumors received [^{3}H]-FAU, 4.2 μCi, by lateral tail vein injection and were euthanized by CO_2 inhalation 4 hours later. Blood was collected into heparinized syringes by cardiac puncture, and a portion was centrifuged at 13,000 × *g* to obtain plasma. The following tissues were immediately removed, weighed, placed on ice, and homogenized in three volumes of phosphate-buffered saline (pH 7.4): liver, kidneys, spleen, heart, lungs, brain, bladder, skeletal muscle, gastrointestinal tract, and tumor. Portions (50–200 μL) of plasma, red blood cells, and tissue homogenates were immediately placed into scintillation vials containing Ready Safe (Beckman Instruments, Fullerton CA). Samples were kept overnight so that chemiluminescence could dissipate before samples were counted. Results of counting were reported as μCi/g tissue or μCi/mL and were normalized to skeletal muscle. Tumor homogenates were analyzed for incorporation of radioactivity derived from FAU into DNA, as described in the next section.

DNA Incorporation of [^{3}H]-FMAU. DNA was extracted from 0.3-mL samples of tumor homogenate, enzymatically digested, and analyzed for thymidine by HPLC and for radioactivity by scintillation counting (9). In our previous report (9), no [^{3}H]-FAU was detected in DNA, and [^{3}H]-FMAU was the only radiolabeled species in the DNA after incubation of cells with [^{3}H]-FAU.

Thymidylate Synthase Catalytic Activity. Three additional mice bearing HT29 and three additional mice bearing LS174T xenografts from the FAU study were euthanized and

Table 1 HT29 or LS174T tumor weights and thymidylate synthase (TS) catalytic activity

Tumor	Tumor weight (g)	TS activity (pmol/min/mg protein)
HT29	1.24 ± 0.16	11.0 ± 1.5
LS174T	2.25 ± 0.92	38.0 ± 4.0*

NOTE. Values are mean ± SD of three tumors.
* Value is different from the value for HT29 tumor; $P \leq 0.01$.

exsanguinated; and their tumors were isolated, weighed, and stored overnight in ice-cold phosphate-buffered saline. The next day, the tumors were analyzed for thymidylate synthase catalytic activity with a [^{3}H]dUMP tritium-release method (10, 11).

PET Imaging. PET scans were acquired in two-dimensional mode with a Siemens/CTI HR+ scanner (Siemens/CTI, Knoxville, TN). The full width at half-maximum resolution of typical reconstructed images is ~6.6 mm in the transverse plane and 5.3 mm in the axial direction when measured as described in Meltzer *et al.* (12).

[^{18}F]-FAU (38 μCi/dose) was administered intravenously to mice anesthetized with 50 mg/kg intraperitoneal pentobarbital (Nembutal Sodium Solution, Abbott Laboratories, North Chicago, IL). Two mice bearing HT29 xenografts and two mice bearing LS174T xenografts were imaged by PET for 90 minutes after administration of [^{18}F]-FAU. For a reference point in the PET images, 5 μCi of the tracer was drawn up into the tips of 1-mL syringes, which were positioned near the tumor of each animal. A 5-minute PET scan was then acquired. A total of 42 emission scans were collected over a period of 90 minutes. The scans were corrected for detector efficiencies, random and scattered coincidences, attenuation, detector dead time, and isotope decay and were reconstructed with a Hann window with the cutoff set to the Nyquist frequency. After acquisition of the PET images, the imaging platform was transferred to an X-ray computed tomography scanner, and a high-resolution (1-mm^3 voxels) image was acquired of the tumor region for each mouse. Computed tomography images were used to guide the placement of the region-of-interest on the PET images to determine the time course of [^{18}F]-FAU uptake in the mice.

Incorporation into DNA *In vitro*. HT29 and LS174T cells were grown in flasks to nearly confluent monolayers. Either [^{3}H]-FAU or [^{3}H]-FMAU (Moravek, Brea, CA) were added at tracer concentrations, in the absence (baseline) or presence of 50 nmol/L 5-fluoro-2′-deoxyuridine (FdUrd). After 3 hours of incubation, cells were washed, scraped from the plates, and digested with trypsin. DNA was extracted and analyzed for radiolabel as described above.

Statistical Analysis. Comparisons between group means and medians were conducted by paired *t* test and Mann-Whitney test, respectively, with the program Minitab (Minitab, State College, PA), and $P \leq 0.05$ was chosen for significance.

RESULTS

Thymidylate synthase activity in the LS174T xenografts was ~3.5-fold higher than that in the HT29 xenografts (Table 1). HT29 xenografts grew more slowly in SCID mice than did LS174T xenografts (median days to one doubling, 9 and 4 days, respectively). Four hours after administration of [^{3}H]-FAU, radioactivity was detected in all tissues (Table 2). No differences were noted in the distribution of radioactivity to normal tissues between mice bearing HT29 tumors or LS174T tumors. Tumor radioactivity was 25% higher in the LS174T tumors than in HT29 tumors, but this difference was not statistically significant. In both tumor types, the tumor-to-muscle ratio was ~2. The radioactivity in plasma was 4-fold higher than that in skeletal muscle. Liver radioactivity was about 3-fold higher than that in skeletal muscle, whereas the radioactivity in the kidneys was only about 1.5-fold higher than that in skeletal muscle. Other tissues contained radioactivity that was less than, or similar to, that measured in skeletal muscle.

[^{3}H]-FMAU incorporation into DNA, reported as ppm, *i.e.*, parts of FMAU per million parts of thymidine, was 2-fold higher ($P \leq 0.01$) in the LS174T tumors than in the HT29 tumors (Table 3).

The whole body image in Fig. 3 shows that radioactivity derived from [^{18}F]-FAU was widely and relatively evenly distributed throughout the mouse, without strong localization in the tumor. The excretion of radioactivity derived from [^{18}F]-FAU in urine is shown by the intensity of the bladder in the PET image. The region-of-interest for tumor measurements was selected based on high resolution computed tomography imaging and palpation of the tumor.

Time courses for ^{18}F radioactivity in tumor and muscle during the 90-minute PET scans of the mice given [^{18}F]-FAU are shown in Fig. 4. Average values are plotted for the two mice bearing HT29 tumors (Fig. 4*A*) and the two mice bearing LS174T tumors (Fig. 4*B*). For comparison, the tumor and skeletal muscle distributions of [^{3}H]-FAU obtained 4 hours after its intravenous administration are included on the same plots. The data are normalized to μCi/g tissue per μCi administered to the animals because in the PET study the mice received ~38 μCi of ^{18}F, whereas in the distribution study, the mice received only 4.2 μCi of ^{3}H. The skeletal muscle concentrations of radioactivity were nearly constant for most of the 90 minutes of PET imaging,

Table 2 Distribution of [^{3}H]-FAU-derived radioactivity in SCID mice bearing HT29 or LS174T xenografts

Tissue	μCi/g tissue or μCi/mL plasma or red blood cells	
	SCID mice with HT29 tumors	SCID mice with LS174T tumors
Tumor	0.083 ± 0.015* (2.39)†	0.104 ± 0.032 (2.28)
Plasma	0.168 ± 0.027 (4.78)	0.160 ± 0.015 (3.74)
Red blood cells	0.033 ± 0.008 (0.94)	0.031 ± 0.007 (0.78)
Liver	0.097 ± 0.038 (2.62)	0.136 ± 0.008 (3.19)
Kidneys	0.078 ± 0.026 (1.42)	0.083 ± 0.046 (1.72)
Spleen	0.043 ± 0.012 (1.23)	0.044 ± 0.003 (1.08)
Heart	0.018 ± 0.002 (0.49)	0.077 ± 0.036 (1.63)
Lungs	0.017 ± 0.001 (0.49)	0.022 ± 0.008 (0.48)
Brain	0.031 ± 0.012 (0.87)	0.021 ± 0.002 (0.51)
Urinary bladder	0.029 ± 0.039 (0.83)	0.029 ± 0.020 (0.81)
Gastrointestinal tract	0.019 ± 0.002 (0.54)	0.020 ± 0.003 (0.48)
Skeletal muscle	0.036 ± 0.008 (1.00)	0.046 ± 0.015 (1.00)

* Mean ± SD of three tumors.
† Values in parentheses are normalized to skeletal muscle.

Table 3 Tumor DNA incorporation of [^{3}H]-FMAUMP derived from [^{3}H]-FAU administered to C.B-17 SCID mice bearing either HT29 or LS174T Xenografts

Tumor type	ppm of thymidine*
HT29	0.023
	0.014
	0.020
	0.019 ± 0.005†
LS174T	0.041
	0.039
	0.044
	0.041 ± 0.003†‡

NOTE. Values provided for each of three individual mice with each tumor.

* Incorporation of radioactivity derived from [^{3}H]-FAU and reported as parts per million (ppm) of thymidine.

† Mean ± SD.

‡ Value is different from the value for HT29 tumor; $P \leq 0.01$.

whereas the tumor concentrations of radioactivity increased throughout the imaging period.

As shown in Fig. 4*C*, the ratio of tumor-to-muscle radioactivity was similar for the two tumor types for the first 35 minutes and then diverged for the remaining 55 minutes because the values for LS174T rose faster than did the values for HT29.

Coincubation of [^{3}H]-FAU *in vitro* with 50 nmol/L FdUrd decreased FAU incorporation into DNA by 70% in HT29 and 84% in LS174T (Table 4). In contrast, a 275% increase was observed for FMAU incorporation in HT29 cells when [^{3}H]-FMAU was coincubated with FdUrd *in vitro*. *In vitro* coincubation of FdUrd with [^{3}H]-FMAU also produced an 891% increase in FMAU incorporation in LS174T cells (Table 4).

DISCUSSION

We proposed that prodrugs such as FAU would be activated to suicide products in tumors with high catalytic activity of thymidylate synthase. In humans, these tumors are generally resistant to thymidylate synthase inhibitors but could be collaterally sensitive to FAU and related compounds. To evaluate this proposal, we wanted cells derived from human tumors, of a type for which thymidylate synthase inhibitors are used clinically.

Human colon cancer was chosen based on the universal use of 5FU in this disease, and the availability of many well-characterized cell lines. Two widely used cell lines, HT29 and LS174T, were chosen because they represented the largest difference, 5-fold, in thymidylate synthase catalytic activity from a panel of 13 colon cancer cell lines evaluated *in vitro* (13). When we grew LS174T and HT29 cells as xenografts in SCID mice, a 3.5-fold difference in catalytic activity was observed between the two xenografts. Sensitivity or resistance to 5FU *in vitro* or *in vivo* was not a selection factor. There are no data on the sensitivity of these cell lines to FAU, either *in vitro* or *in vivo*.

Preclinical studies suggest that FAU has pharmacokinetic properties that should facilitate its development. Studies with [^{18}F]-FAU tracer doses in normal dogs demonstrated that, at 4 hours after administration of the tracer, tissue-to-blood ratios were close to 1 and that the tracer distributed evenly to organs not involved in the clearance of FAU (14). There was no accumulation of FAU radioactivity in bone marrow. The urinary bladder and gall bladder, each a repository for excretion, contained high levels of radioactivity, and 95% of the radioactivity in urine was FAU (14). Continuous infusion of FAU in dogs for 5 days was well tolerated, and plasma concentrations of FAU could be sustained at the concentration targets established *in vitro* (15). Furthermore, after oral administration to dogs, 74 to 99% of the FAU was bioavailable (16). Traditionally, the next step in the development of a therapeutic agent would be a demonstration in tumors *in vivo* that the molecular characteristics and/or antitumor activity were consistent with the underlying concept. The results from these *in vivo* studies of human colon cancer xenografts provide an essential bridge along the path between the development *in vitro* of the concept of prodrugs activated by thymidylate synthase and the ultimate clinical evaluation of this concept.

It is well established that the high concentration of circulating thymidine in murine plasma (including that of SCID mice) reduces the utility of murine models for assessment of thymidylate synthase as a target for chemotherapy because circulating thymidine provides a "rescue" pathway that permits continued synthesis of DNA despite inhibition of thymidylate synthase (17). For prodrugs activated by thymidylate synthase, the high circulating thymidine may compete for prodrug acti-

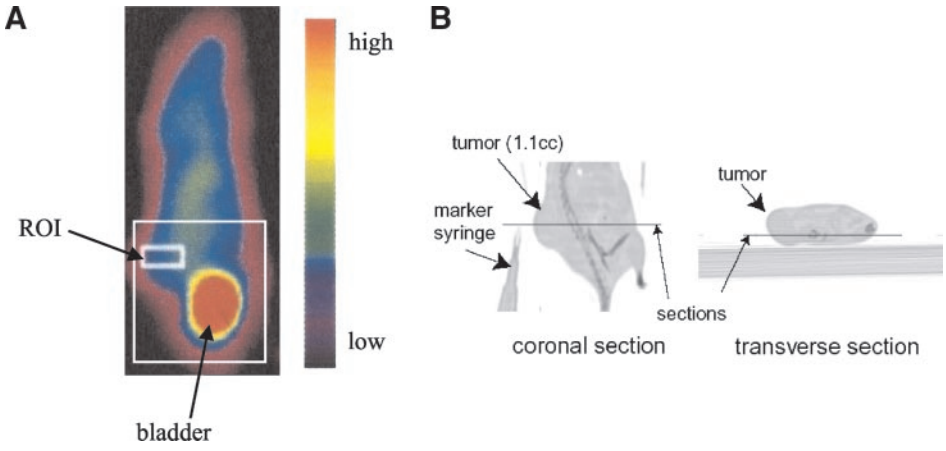

Fig. 3 PET image of a mouse given [^{18}F]-FAU and bearing HT29 tumor in the region-of-interest (*ROI*). *A*, the (*scale on the right*) relates concentration of total radioactivity to the color scheme in the image. Most of the radioactivity was contained in the urinary bladder, as a consequence of excretion of radioactivity derived from [^{18}F]-FAU. *B*, computed tomography images of the same mouse.

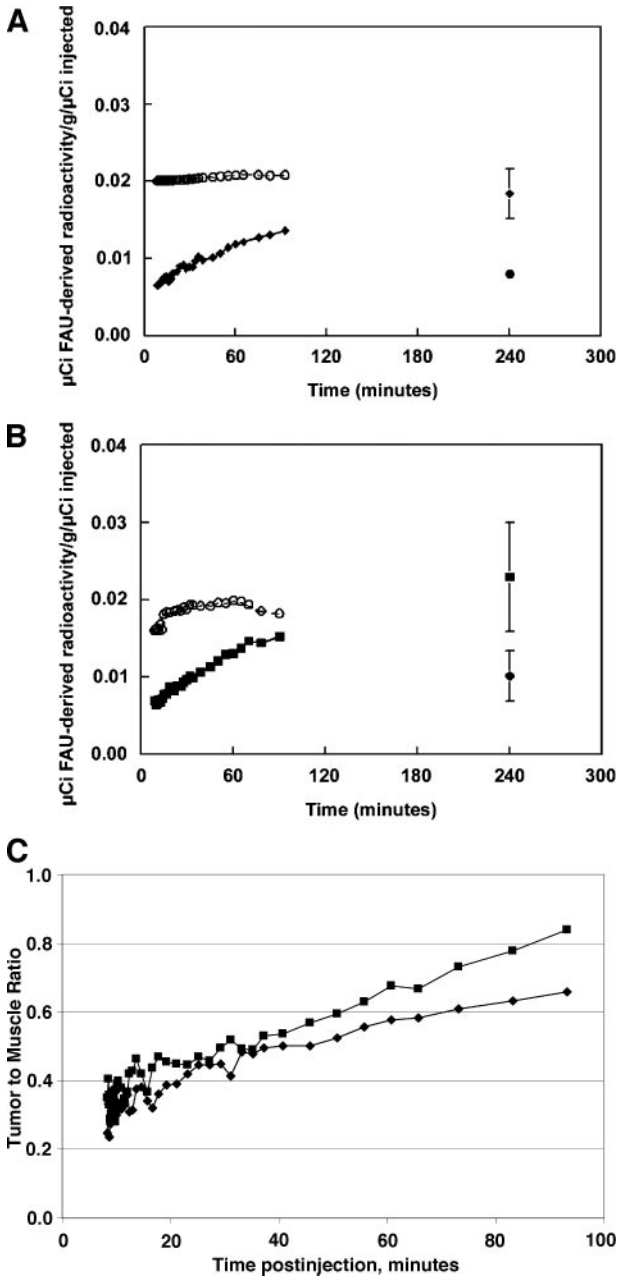

Fig. 4 Biodistribution of radiolabeled FAU in mice. *A*, [^{18}F]-FAU-derived radioactivity *versus* time for skeletal muscle (*circles*) and HT29 tumors (*diamonds*) over 90 minutes, compared with [^{3}H]-FAU-derived radioactivity obtained at 240 minutes. *B*, corresponding data for skeletal muscle (*circles*) and LS174T tumors (*squares*). *C*, comparison of tumor-to-muscle ratios for the two tumor types during the 90-minute time course of monitoring radioactivity derived from [^{18}F]-FAU. ▨, LS174T tumor-to-muscle ratio; ♦, HT29 tumor-to-muscle ratio.

vation by thymidine kinase. We expect that conventional antitumor activity studies would not be feasible because of competition from thymidine, but we are not aware of any published studies of FAU antitumor activity *in vivo*.

By analogy to behavior in cell culture, we expect that the absolute values for DNA incorporation of methylated drug are also reduced by competition from thymidine. However, the rank order for incorporation into DNA remains useful as an end point for pivotal development decisions such as the selection of one analog *versus* another. Also, as shown in this study, comparison of relative incorporation into DNA of tumors with different catalytic activity of thymidylate synthase provides verification *in vivo* of the previous findings *in vitro*. Thus, if conventional antitumor activity studies are not feasible, molecular pharmacological end points such as DNA incorporation of methylated drug become pivotal end points for development decisions.

Recently, Wang *et al.* (18) reported that [^{14}C]-FAU can be methylated by thymidylate synthase and incorporated as FMAU into the DNA of CEM tumors growing in SCID mice. The actual amounts of FAU in DNA were low. A number of factors contribute to low incorporation in DNA, including the short exposure time to the probe, small amounts of DNA that were synthesized during the interval, and, presumably, competition from circulating thymidine. Nonetheless, as the first demonstration *in vivo* of the biochemical events shown in cell culture, these results provide general support for the thymidylate synthase prodrug concept.

Our report links relatively small differences in thymidylate synthase catalytic activity (3.5-fold) to quantitative differences in DNA incorporation of FMAU derived from FAU. These differences were statistically significant, despite the small numbers of animals. Because there are many steps required between dosing of FAU and incorporation into DNA as FMAU, it must be established that thymidylate synthase is a critical step. Also, there is a need to understand whether small differences in thymidylate synthase activity can be measured, or whether very large differences (*e.g.*, 10-fold or greater) are required to visualize changes in thymidylate synthase catalytic activity. Thus, the association reported in this work between thymidylate synthase catalytic activity and incorporation of [^{3}H]-FMAU into DNA of LS174T and HT29 tumors provides substantial biochemical support for the concept that tumors with high thymidylate synthase catalytic activity can be selectively targeted for therapy with prodrugs activated by thymidylate synthase. Unfortunately, immunohistochemistry data for thymidylate synthase in patient tumors are not directly comparable with enzyme activity data obtained from these xenografts.

Experiments in cell culture can help to determine whether steps before thymidylate synthase (transport across the cell membrane and phosphorylation by thymidine kinase) or subsequent to thymidylate synthase (adding additional phosphate groups and DNA polymerization) were controlling factors for the rate of FAU incorporation into DNA. If any of these factors were dominant, then changes in the activity of thymidylate

Table 4 Percentage change in incorporation of ^{3}H-nucleoside into DNA when cells are coincubated with FdUrd (50 nmol/L) compared with baseline incorporation in the absence of FdUrd

	% change in incorporation	
Cell line	[^{3}H]-FAU (43 nmol/L)	[^{3}H]-FMAU (159 nmol/L)
HT29	−70	275
LS174T	−84	891

synthase as monitored by FAU would be obscured. In particular, the rate of phosphorylation of FAU is reported (14) to be relatively poor as a percentage of thymidine phosphorylation, 0.4%.

At nanomolar concentrations in extracellular fluid, FdUrd selectively inhibits thymidylate synthase without any reported influence on transport, kinases, or polymerases. Thus, coincubation of FdUrd with FAU would be expected to inhibit thymidylate synthase and prevent accumulation of FAU in DNA. The 70–80% decreases in incorporation that were observed with FdUrd in this study are consistent with the scenario that thymidylate synthase activity is a major determinant for incorporation of FAU into DNA.

However, if FdUrd decreased DNA synthesis, then it would not be possible to distinguish whether the impact of FdUrd was due to specific blockade of thymidylate synthase or due to a general effect of a lower rate of DNA synthesis. We used [^{3}H]-FMAU incubations *in vitro* to help evaluate the possibilities. The incorporation of FMAU into DNA follows a pathway identical to FAU, except that thymidylate synthase is not required. Thus, as a control, incorporation of FMAU into DNA was studied in the absence and presence of FdUrd. If FdUrd acted by stopping DNA synthesis, then the incorporation of FMAU into DNA would be decreased. On the other hand, if FdUrd specifically blocked thymidylate synthase, then the cell would increase its reliance on the salvage pathway and FMAU incorporation into DNA would increase. The latter possibility is strongly supported by the 3- to 9-fold increases of FMAU incorporation into DNA that were observed in these studies. Wells *et al.* (19) have reported the use of increased uptake of radiolabeled thymidine as an indirect probe for thymidylate synthase.

Taken together, these observed increases in FMAU incorporation, when combined with the decreases observed for FAU incorporation, help to rule out other explanations and strengthen the interpretation that thymidylate synthase is the most important determinant for incorporation of FAU into DNA.

In addition to interest in therapeutic applications of prodrugs activated by thymidylate synthase, there is also considerable practical value in combining such an approach with external imaging to help guide selection of therapy based on the extent of phenotypic thymidylate synthase expression, *i.e.*, catalytic activity. For this application, the results from our work are encouraging but mixed. The whole body PET image is based on total radioactivity but is consistent with prior reports in dogs (14) that FAU is not substantially metabolized and is excreted unchanged in the urine. Although the incorporation of radiolabel into DNA is the key condition related to cytotoxicity, external imaging measures total radioactivity and not a specific compound. For FAU, the radiolabeled species include the parent compound, its monophosphate (FAUMP), methylated nucleotides, and DNA.

Although potentially beneficial, it was unexpected that the tumor localization would continue to increase during the entire 90-min imaging period. These PET imaging results can be interpreted as a delay in the removal of nonspecific ^{18}F radioactivity from the body, followed by a period in which differences in activated ^{18}F-species were more apparent.

It might have been expected that, over time, differential accumulation would be magnified as the radiolabel in DNA persists and the unincorporated radiolabel is washed out of tissues. This pattern was observed when tumor and muscle radioactivity at 4 hours after administration of [^{3}H]-FAU was compared with accumulation of radioactivity via ^{18}F PET imaging at 90 minutes. However, we expected substantial differences between tumors with high and low thymidylate synthase expression, but the observed differences in total radioactivity were small and not statistically significant.

Interpretation of data from the murine model used in these studies and extension of these data to the clinical situation need to be tempered by differences in competing thymidine concentrations between humans and mice (17) and the lack of specificity of total radioactivity as an analytical probe. Future studies will need to examine a wider range of thymidylate synthase catalytic activity as part of the probe concept validation and should also consider evaluation of probe behavior when an inhibitor of thymidylate synthase, *e.g.*, 5FU, is used.

In general, probes with high specific localization within tumors are desired. For example, [^{18}F]fluorodeoxyglucose has been highly successful because its tumor-to-background ratio is in the range of 5 to 10. When examining an [^{18}F]fluorodeoxyglucose PET image, the tumor is readily observed because of this high contrast in uptake. In this study, we did not observe high localization of [^{18}F]-FAU in tumors compared with background. Although desirable, high values for tumor-to-background ratios are not an absolute requirement. With quantitative visualization of three-dimensional images, and increasing clinical use of the PET-computed tomography hybrid scanner in the clinic (20), other techniques can establish the anatomic location of the tumor, whereas PET can focus on the biochemical pattern.

ACKNOWLEDGMENTS

We thank Dr. Thomas Mangner of Wayne State University for many helpful comments regarding the synthesis of [^{18}F]-FAU, and Dr. Anthony Shields of Wayne State University for his encouragement and insights into FAU studies. We thank the "UPCI Hematology/Oncology Writing Group" for their helpful review and Ezekiel Woods for excellent secretarial support. We also thank Diane Mazzei and her coworkers in the University of Pittsburgh Animal Facility for their expert assistance.

REFERENCES

1. Devita VT, Hellman S, Rosenberg SA, editors. Cancer: principles and practice of oncology, 6th ed. Philadelphia: Lippincott Williams & Wilkins; 2001.

2. Ichikawa W, Uetake H, Shirota Y, et al. Combination of dihydropyrimidine dehydrogenase and thymidylate synthase gene expressions in primary tumors as predictive parameters for the efficacy of fluoropyrimidine-based chemotherapy for metastatic colorectal cancer. Clin Cancer Res 2003;9:786–91.

3. Allegra CJ, Paik S, Colangelo LH, et al. Prognostic value of thymidylate synthase, Ki-67, and p53 in patients with Dukes' B and C colon cancer: a National Cancer Institute-National Surgical Adjuvant Breast and Bowel Project collaborative study. J Clin Oncol 2003;21:241–50.

4. Kralovanszky J, Koves I, Orosz Z, *et al.* Prognostic significance of the thymidylate biosynthetic enzymes in human colorectal tumors. Oncology 2002;62:167–74.

5. Aschele C, Lonardi S, Monfardini S. Thymidylate synthase expression as a predictor of clinical response to fluoropyrimidine-based chemotherapy in advanced colorectal cancer. Cancer Treat Rev 2002;28:27–47.

6. Collins JM, Klecker RW, Katki AG. Suicide prodrugs activated by thymidylate synthase: rationale for treatment and noninvasive imaging of tumors with deoxyuridine analogues. Clin Cancer Res 1999;5:1976–81.

7. Mangner TJ, Klecker R, Anderson L, Shields AF. Synthesis of 2′-deoxy-2′-[18F]fluoro-beta-D-arabinofuranosyl nucleosides, [18F]FAU, [18F]FMAU, [18F]FBAU and [18F]FIAU, as potential PET agents for imaging cellular proliferation. Synthesis of [18F]labelled FAU, FMAU, FBAU, FIAU. Nucl Med Biol 2003;30:215–24.

8. Hamacher K, Coenen HH, Stocklin G. Efficient stereospecific synthesis of no-carrier added 2-[F-18]-fluoro-2-deoxy-D-glucose using aminopolyether supported nucleophilic substitution. J Nucl Med 1986; 27:235–8.

9. Klecker RW, Katki AG, Collins JM. Toxicity, metabolism, DNA incorporation with lack of repair, and lactate production for 1-(2′-fluoro-2′-deoxy-β-D-arabinofuranosyl)-5-iodouracil in U-937 and MOLT-4 cells. Mol Pharmacol 1994;46:1204–9.

10. Armstrong RD, Diasio RB. Improved measurement of thymidylate synthetase activity by a modified tritium-release assay. J Biochem Biophys Methods 1982;6:141–7.

11. Speth PAJ, Kinsella TJ, Chang AE, Klecker RW, Belanger K, Collins JM. Selective incorporation of iododeoxyuridine into DNA of hepatic metastases versus normal human liver. Clin Pharmacol Ther 1988;44:369–75.

12. Meltzer CC, Kinahan PE, Greer PJ, Nichols TN. Comparative evaluation of MR-based partial-volume correction schemes for PET. J Nucl Med 1999;40:2053–65.

13. van Triest B, Pinedo HM, van Hensbergen Y, *et al.* Thymidylate synthase level as the main predictive parameter for sensitivity to 5-fluorouracil, but not for folate-based thymidylate synthase inhibitors, in 13 nonselected colon cancer cell lines. Clin Cancer Res 1999;5:643–54.

14. Sun H, Collins JM, Mangner TJ, Muzik O, Shields AF. Imaging [18F]FAU [1-(2′-deoxy-2′-fluoro-beta-D-arabinofuranosyl) uracil] in dogs. Nucl Med Biol 2003;30:25–30.

15. Lin T, Chang CJG, Noker PE, Smith AC, Page JG. Disposition of 2′-flouro-ara-deoxyuridine (FAU, NSC-678515) in beagle dogs [abstract]. Proc Am Assoc Cancer Res 2000;41:703.

16. Chang CJG, Smith AC, Fulton R, *et al.* 120-hour infusion dose range-finding study of 2′-flouro-ara-deoxyuridine (FAU, NSC-678515) in beagle dogs [abstract]. Proc Am Assoc Cancer Res 2000;41:703.

17. Jackman AL, Taylor GA, Calvert AH, Harrap KR. Modulation of anti-metabolite effects. Effects of thymidine on the efficacy of the quinazoline-based thymidylate synthetase inhibitor, CB3717. Biochem Pharmacol 1984;33:3269–75.

18. Wang H, Oliver P, Nan L, et al. Radiolabeled 2′-fluorodeoxyuracil-beta-D-arabinofuranoside (FAU) and 2′-fluoro-5-methyldeoxyuracil-beta-D-arabinofuranoside (FMAU) as tumor-imaging agents in mice. Cancer Chemother Pharmacol 2002;49:419–24.

19. Wells P, Aboagye E, Gunn RN, et al. 2-[11C]thymidine positron emission tomography as an indicator of thymidylate synthase inhibition in patients treated with AG337. J Natl Cancer Inst (Bethesda) 2003;95: 675–82.

20. Kluetz PG, Meltzer CC, Villemagne VL, et al. Combined PET/CT imaging in oncology. Impact on patient management. Clin Positron Imaging 2000;3:223–30.